

Article

Potential Use of Residual Sawdust of *Eucalyptus globulus* Labill in Pb (II) Adsorption: Modelling of the Kinetics and Equilibrium

Candelaria Tejada-Tovar ¹, Angel Villabona-Ortiz ¹, Rodrigo Ortega-Toro ^{2,*}, Humberto Mancilla-Bonilla ³ and Fran Espinoza-León ³

¹ Process Design and Biomass Utilization Research Group (IDAB), Chemical Engineering Department, Universidad de Cartagena, Avenida del Consulado St. 30, Cartagena de Indias 130015, Colombia; ctejadat@unicartagena.edu.co (C.T.-T.); avillabonao@unicartagena.edu.co (A.V.-O.)

² Food Packaging and Shelf Life Research Group (FP&SL) and Complex Fluids Engineering and Food Rheology Research Group (IFCRA), Department of Food Engineering, Universidad de Cartagena Avenida del Consulado St. 30, Cartagena de Indias 130015, Colombia

³ Department of Architecture and Engineering, Universidad Nacional del Centro del Perú, Mariscal Castilla 3909, Huancayo 12006, Peru; hbonilla@uncp.edu.pe (H.M.-B.); e_2010100081J@uncp.edu.pe (F.E.-L.)

* Correspondence: rortegap1@unicartagena.edu.co

Abstract: The raw sawdust of *Eucalyptus globulus* Labill was studied as an alternative of residual biomaterial for the adsorption of lead (II) in wastewater, evaluating the effect of pH (3, 4, 5, and 6) in a batch system. From the characterization of the biomaterial, it was found that the biomass has a low ash content, and from the scanning electron microscopy (SEM) microphotographs that it presents a porous morphology with diverse texture and presence of fiber fragments, which describe the heterogeneity of the material. The Fourier transform infrared (FTIR) spectrum showed the presence of functional groups of NH_R, OH, COOH, and hydrocarbons, which are part of the structure of lignin, cellulose, hemicellulose, and pectin. From the adsorption experiments, it was obtained that the optimal value of pH 6, reaching a removal percentage of 96% and an adsorption capacity of 4.80 mg/g. The model that better adjusted the kinetics results was the pseudo-second-order model and the Langmuir and Freundlich isothermal models described the adsorption equilibrium; it was found that in the system prevails chemisorption, supported in ion exchange by Pb (II) and the biomass' functional groups. From the results, eucalyptus sawdust is suggested as a low-cost adsorbent for Pb (II) bioadsorption present in solution.

Keywords: bioadsorption; kinetics; isotherms; lead (II)



Citation: Tejada-Tovar, C.; Villabona-Ortiz, A.; Ortega-Toro, R.; Mancilla-Bonilla, H.; Espinoza-León, F. Potential Use of Residual Sawdust of *Eucalyptus globulus* Labill in Pb (II) Adsorption: Modelling of the Kinetics and Equilibrium. *Appl. Sci.* **2021**, *11*, 3125. <https://doi.org/10.3390/app11073125>

Academic Editor: Chang Geun Yoo

Received: 15 February 2021

Accepted: 25 March 2021

Published: 1 April 2021

Publisher's Note: MDPI stays neutral with regard to jurisdictional claims in published maps and institutional affiliations.



Copyright: © 2021 by the authors. Licensee MDPI, Basel, Switzerland. This article is an open access article distributed under the terms and conditions of the Creative Commons Attribution (CC BY) license (<https://creativecommons.org/licenses/by/4.0/>).

1. Introduction

The presence of metallic ions in water bodies has become an environmental problem of great interest for the scientific community, regarding toxicity and effects on aquatic fauna and people's health [1]. Lead (Pb²⁺) is considered a hazardous pollutant [2], and its main sources of release include fossil fuel combustion, sulfide ore smelting, mining, agriculture, battery, paint, welding, piping, plating, pulp, and paper manufacturing [3]. Lead causes sterility, abortions, neonatal mortality, kidney disease, and mental disorders, and the World Health Organization (WHO) established maximum allowable limits in waters of 0.01 mg/L [4].

Several studies have reported the effect of metallic ions on human health, resulting in the implementation of new technologies for the elimination of these pollutants on wastewaters that are environmentally friendly, with low energy consumption [5]. Physicochemical processes, like adsorption, chemical precipitation, ion exchange membrane technology, electrochemical treatment, and oxidative processes [6], have been widely implemented in the decontamination of water loaded with heavy metals. These methods are expensive and

inefficient at high concentrations [7]. Currently, adsorption is considered as a good method for the removal of a wide spectrum of toxic substances—like heavy metals and emerging contaminants—from wastewaters [8]. Bioadsorption uses lignocellulosic residues, which are cheap and highly available, and could be useful in the treatment of effluents [9]. Other merits of the biosorption method include the reuse of used biosorbents, the short operating time, and the absence of production of secondary contaminants [6].

Recently, many inert-biomass-derived adsorbents have been studied for water cleaning; postharvest and agro-industrial residues have been studied for this purpose. Agricultural waste such as tea residues [10], coffee residues [11], kenaf [12], coconut fiber [13], Japanese loquat [14], and orange peel [15] have shown good performance under the different conditions evaluated due to their lignocellulosic nature which guarantees the presence of functional adsorption groups [16], proving that forest residues are a good biomaterial font for the elimination of metallic ions in solution [17]. The use of bioadsorbents of residual lignocellulosic origin has advantages, such as low cost, high availability, and excellent performance at high and low concentrations [18]. There are many forestall residues used as heavy metal adsorbent, including pine [19,20], picea from Afghanistan [17], poplar wood sawdust [21], *Leucaena leucocephala* [22], and many others, finding that sawdust residues show great skills in wastewater treatment because they are abundantly available and cheap [23].

The *Eucalyptus globulus* Labill (Myrtaceae) is the forest species with the highest production in the Peruvian central highlands for around 100 years, with a production around 68,089.26 m³ of sawn wood and 526,350 m³ of roundwood [24]. Due to the high production of this species and its high logging in Peru [25], a large amount of residual material such as sawdust is produced. In this sense, the objective of this study is to investigate the viability of forest and industrial waste product in its natural form as an adsorbent for the elimination of Pb (II). The waste product investigated is sawdust from native *Eucalyptus globulus* Labill, determining the effect of pH on the adsorption capacity of the biomaterial in batch system. The best fit to the kinetic (pseudo-first order, pseudo-second order, Elovich, and intra-particle diffusion) and isothermal (Langmuir and Freundlich) models was investigated. Sawdust was characterized by ash content determination, scanning electron microscopy (SEM) and Fourier transform infrared spectroscopy (FTIR).

2. Materials and Methods

2.1. Materials and Reagents

Lead nitrate (Pb(NO₃)₂) of 99.5% purity Merk Millipore brand was used for the experimental development of this study. For the characterization of the biomaterial, a Zeiss Scanning Electronic Microscope model EVO 10Z6 with acetylene/air flame was used, and a BET equipment model Gemini VII 2390 Surface Area Analyzer and Porosity was used. The remaining metal concentration in the solution was determined by atomic absorption using atomic absorption spectrophotometer brand Perkin Elmer model 969 Solar series with flame. The tests in the batch system were carried out in a circular shaker made by Aros 160 Termolyne model No. M660 20-26.

2.2. Preparation of the Bioadsorbent

Two kilograms of eucalyptus sawdust was collected as forestry waste in the district of Huancayo, Peru. The material was then washed, dried for 15 h, pulverized and homogenized in a mortar, and stored in airtight bags to keep it in good condition. The sawdust was characterized by determining the ash content, and Fourier transform infrared spectroscopy (FTIR) analysis was used to study the surface chemistry and evaluate the functional groups of the sawdust. Scanning electron microscopy analysis was made to gauge the superficial morphology of the sawdust, using 2 mg of sawdust powder coated with 1 md gold.

2.3. Pb (II) Adsorption Experiments

The completely randomized experimental design was used in which the pH was varied in four levels (3, 4, 5, and 6) with four replicates, for a total of 16 experiments. For the adsorption tests, 50 mL of solution with an initial concentration of 150 mg/L of contaminant with 1.5 g of sawdust, was placed in contact, shaking 180 rpm, at 20 °C, under the different pH conditions considered for 30 min. The pH was regulated with 0.01 M HCl and 0.01 M NaOH solutions using a Handylab Ph 11 pH meter. Atomic absorption at 217 nm was used in the determination of the equilibrium concentration. The efficiency and adsorption capacity were calculated according to Equations (1) and (2):

$$\%E = \frac{(C_0 - C_e)}{C_0} \times 100 \quad (1)$$

$$q_e \left(\frac{\text{mg}}{\text{g}} \right) = \frac{(C_0 - C_e) \times V}{m} \quad (2)$$

where %E is the adsorption efficiency, q_t is the adsorption capacity in mg/g, C_0 and C_e are the initial and equilibrium concentration in mg/L, of the solution to be adsorbed V the volume in L and m the mass of adsorbent in g.

2.4. Kinetics and Isotherms of Adsorption

The kinetic was studied at the best pH condition found, by placing in contact 100 mL of a synthetic solution of Pb (II) at 150 mg/g with 1.5 g of sawdust at 20 °C and 180 rpm. Samples were taken at different time intervals (3, 5, 10, 20, 30, 50, 60, 90, 120 min). The amount of metal remaining in the solution was determined by atomic absorption at 217 nm. The experimental data obtained were modelled with the non-linear equations of pseudo-first-order, pseudo-second-order, Elovich, and intraparticle diffusion, in order to establish the stages that control the process (Table 1).

Table 1. Kinetic models [26].

Model	Equation	Parameter
Pseudo-first-order	$q_t = q_e (1 - e^{-k_1 t}) \quad (1)$	q_e and q_t (mg/g): adsorption capacities in equilibrium and at a certain time. k_1 (min ⁻¹): Constant of Lagergren.
Pseudo-second-order	$q_t = \frac{t}{\frac{1}{k_2 q_e^2} + \frac{t}{q_e}} \quad (2)$	k_2 (g ⁻¹ min ⁻¹): pseudo-second-order adsorption constant.
Elovich	$q_t = \frac{1}{\beta} \ln(\alpha\beta) + \frac{1}{\beta} \ln(t) \quad (3)$	α (mg·g ⁻¹ ·min ⁻¹): initial speed of adsorption. β (g·mg ⁻¹): desorption constant related to surface range, and activation energy for chemisorption. q_t (mg/g): the amount of chemisorbed metal.
Intraparticle diffusion	$q_t = k_3^{1/2} t \quad (4)$	q_t (mg/g): quantity of metal adsorbed per mass unit of adsorbent in a time t . t (min): is the time. k_3 (mg·g ⁻¹ ·min ^{-1/2}): constant intraparticle diffusion.

The isotherm of adsorption was determined in order to study the effect of the initial concentration over the process and to establish the driving forces involved in adsorption [27]. For this, the experiments were carried out at different initial concentrations of sorbate (30, 60, 90, 120, and 150 mg/L) using 1.5 g of sawdust, at 180 rpm, room temperature, for 24 h at the different pH values evaluated. The experimental data were adjusted to Langmuir and Freundlich's models (Table 2).

Table 2. Isothermal models.

Model	Equation	Parameters
Langmuir	$q_t = q_{\max} \frac{K_L C_f}{1 + K_L C_f}$	<p>q_t (mg/g): is the amount of metal adsorbed on the bioadsorbent.</p> <p>C_f (mg/L): residual metal concentration in solution.</p> <p>q_{\max} (mg/g): maximum adsorption capacity of the Langmuir model.</p> <p>K_L: is Langmuir's constant and can be correlated with the variation of the adsorption area and the porosity of the adsorbent.</p>
Freundlich	$q_t = k_f C_e^{1/n}$	<p>k_f (L/g): Freundlich's constant and represents the distribution coefficient.</p> <p>n (mg/g): represents the adsorption intensity and indicates the heterogeneity of the active sites.</p> <p>q_t (mg/g): the amount of metal adsorbed at equilibrium.</p> <p>C_e (mg/L): residual concentration of the metal in solution.</p>

3. Results

3.1. Characterization of Sawdust

An ash and dry matter content of 1.552% was obtained, which guarantees that the biomass obtained is of good quality and does not contain heavy metals in its structure [28]. This ash content may be due to the presence of aluminum oxides, silica, calcium, magnesium, and iron in its structure, which could function as active centers of adsorption [29].

SEM microphotographs of eucalyptus sawdust at 20 and 50 μm magnification, taken to show the variation in shape and superficial texture of the adsorbent [19], are shown in Figure 1. A widely heterogeneous structure is observed with the presence of fiber fragments, blocks with appreciable and irregular circular indentations, heterogeneous spirals, fragments embedded square grids, heterogeneous spirals, and very pronounced pores forming porous structures, which contribute to augment the area of contact. The fiber fragments shown are due to the presence of cellulose, hemicellulose, and lignin in the sawdust's structure, which benefits the adsorptive capacities of the material due to the presence of COOH, NH_R , and OH groups, which have the capacity to retain Pb (II) ions with the formation of the complex [30]; The presence of pore formation, which is a mechanism of Pb (II) adsorption, was also observed.

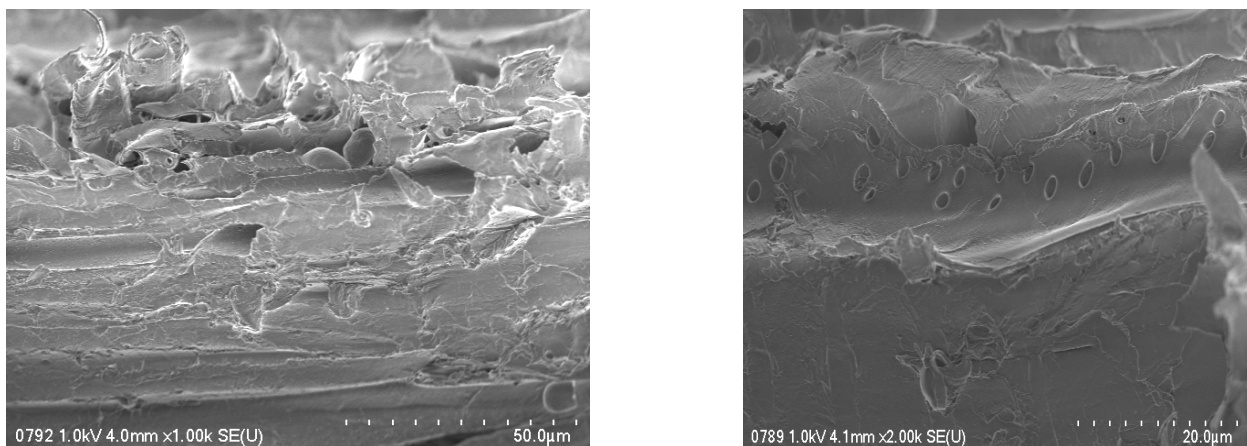


Figure 1. Scanning electron microscopy (SEM) microphotographs of eucalyptus sawdust.

The FTIR analysis of the eucalyptus sawdust before and after the adsorption (Figure 2) was performed to know the surface chemistry of the biomass and to establish the functional groups present in the structure of the biomaterial and involved in the uptake of the

metal [31]. In the spectrum of unsaturated eucalyptus a high intensity peak at 3391.94 cm^{-1} was identified as related to the stretching of the O-H group present in the phenolic and carboxylic structure [27]; the widening and symmetry of this band indicates the presence of strong hydrogen bonds, corresponding to the pectin functional groups [32]. The bands 2918.85 cm^{-1} , 2847.49 cm^{-1} , and 2515.04 cm^{-1} are related to the stretching of the C-H bond present in aromatic rings, corresponding to the functional groups of cellulose and lignin [33]; the signals 1651.76 cm^{-1} , and 1514.51 cm^{-1} correspond to the stress C=C, present in aromatic rings corresponding to the lignin functional groups [34]. The high-intensity peaks at 1454.35 cm^{-1} and 1424.18 cm^{-1} show the C-H deformation corresponding to the hemicellulose functional groups [35]. The wavenumber 1384.69 cm^{-1} corresponds to the stretching of C=C, characteristic of polyaromatics, and assigned to the stretching of C-O-C bonds type of carboxylic acids and carboxylates, corresponding to the functional groups of cellulose [36]; the 1233.88 cm^{-1} signal shows the C-O bond, present in alcohols and carboxylic acids, corresponding to the functional groups of lignin [37]; the 1036.50 cm^{-1} band shows the C-O elongation of carboxylics [37], in the band 873.29 cm^{-1} corresponds to the C-C stretch, in the signals from 776.78 cm^{-1} to 656.46 cm^{-1} have C-Cl links, in the bands, 559.75 cm^{-1} and 539.31 cm^{-1} correspond to the C-Br links and finally, 470.79 cm^{-1} and 415.63 cm^{-1} are assigned to the C-I link [28].

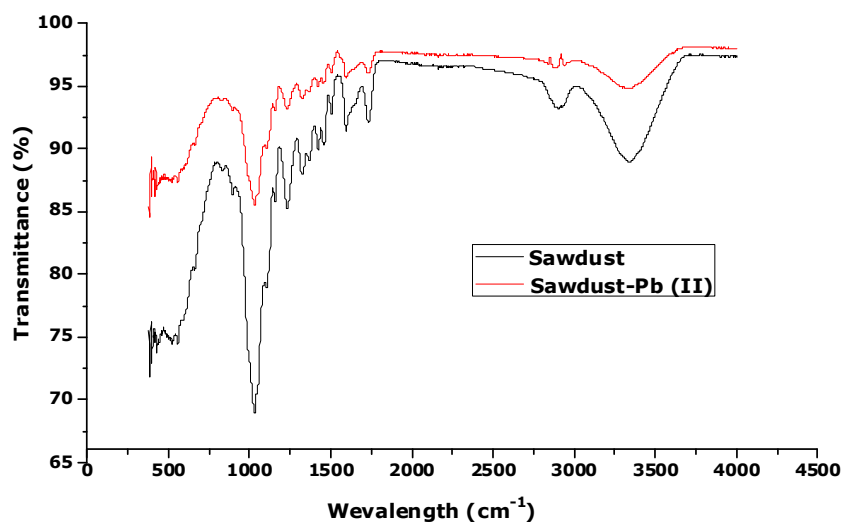


Figure 2. Infrared (IR) spectrum of eucalyptus sawdust before and after Pb (II) adsorption.

After Pb (II) adsorption the previously mentioned bands show a decrease in their intensity due to the bonding of the metal to these by physical interactions through London or Van der Waals force or by chemical bonding through ion exchange or covalent bonds between the adsorbent and the adsorbate forming complexes [36]. In the different IR spectra of eucalyptus sawdust, considering the signals from 3391.94 cm^{-1} to 1036.50 cm^{-1} correspond mostly to the functional groups present in the structure of biopolymers such as pectin, cellulose, hemicellulose, and lignin, which are found inside the cell walls of the adsorbent [35]; these functional groups (carboxyl, amino, and hydroxyl) function as active binding sites capable of sequestering Pb (II) ions [38]. We found shifting of the peaks 2361.19 cm^{-1} ($\text{C}\equiv\text{N}$), 1650.45 cm^{-1} (C=C), 3390 cm^{-1} (NH), 3391.94 cm^{-1} (OH), and 1156.55 cm^{-1} (sulfonamides). That phenomenon is attributed to the linking between the heavy metal and the active sites present in the sawdust [32].

3.2. Effect of pH

pH of the solution is an important factor in the metal adsorption process, because it impacts the surface chemistry of the bioadsorbent, speciation, sequestration, and mobility of metal [39]; the effect of pH variation (3, 4, 5, and 6) on the Pb (II) removal process on eucalyptus sawdust was investigated. This pH range was selected because, according to

the speciation graph of Pb (II) in water [40], when $\text{pH} > 6$ the Pb^{+2} species begins to convert into other species such as $\text{Pb}(\text{OH})_2$, $\text{Pb}(\text{OH})_3^-$, $\text{Pb}(\text{OH})_4^{+2}$, PbNO_3^+ , PbOH , which are found in a low proportion between pH 3 to 6 [41]. Figure 3 shows the average of the pH data with respect to the adsorption capacity of Pb (II) on the eucalyptus sawdust, finding that the highest adsorption capacity is 4.80 mg/g obtained at pH 6, achieving a removal efficiency of 96.01%. This can be explained by the fact that as the surface charge of the biomass became more negative proportionally with the pH , the adsorption of the metal increased too, since the negative surface charge leads to the deprotonation of functional groups in the sawdust. Therefore, the deprotonated active sites, are easily accessible to the ions, increasing the adsorption rate [42]. At low pH 's, the repulsion between the ions and positively charged exchange sites occur along with competition with H_3O^+ , which prevents the ions from being successfully captured [43]. Above pH 6, considering lead speciation, low solubility hydroxides such as $\text{Pb}(\text{OH})_2$ are formed, so adsorption at higher pH s would be difficult, as reported [43].

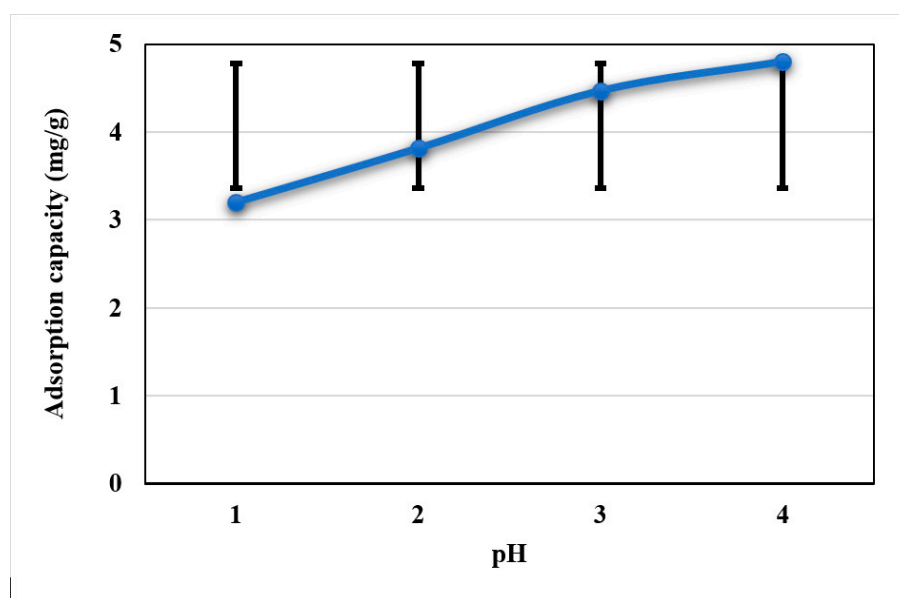


Figure 3. Effect of pH variation on the adsorption capacity of Pb (II).

Similar results to this study have been obtained when using rice straw [44], oil palm fiber residues [45], avocado shells [30]. Studies report that by increasing the pH to 6, due to the fact that ion exchange is the process that dominates the removal of the metal and at low pH s the surface of the metal is protonated by H_3O^+ ions, which compete for the active sites with the lead ions and by having greater mobility and preference for adsorption at the surface they decrease the adsorption capacity of the ion in the adsorbent [46]. As the pH increases, the negative charge density in the biosorbent increases due to the deprotonation of the metal-binding sites; this phenomenon increased the biosorption of the metal [47].

Pb (II) adsorption capacities have been achieved between 3.9 and 8.9 mg/g on biomass of the fungus *Lepiota hystrix* [48], 12.86 mg/g on a bio-adsorbent from *Lavan-dula pubescens Decne* [49], 82.24 mg/g, 91.12 mg/g, 99.19 mg/g, and 40.41 mg/g on yam, banana, cassava, and oil palm bagasse shells, respectively [32], and 0.112 mg/g on residual mushroom biomass [50]. It is observed that the results obtained in the present study are in the range of 0.1–99 mg/g reported in the literature, so it can be said that eucalyptus sawdust is a good source for the preparation of bioadsorbent material.

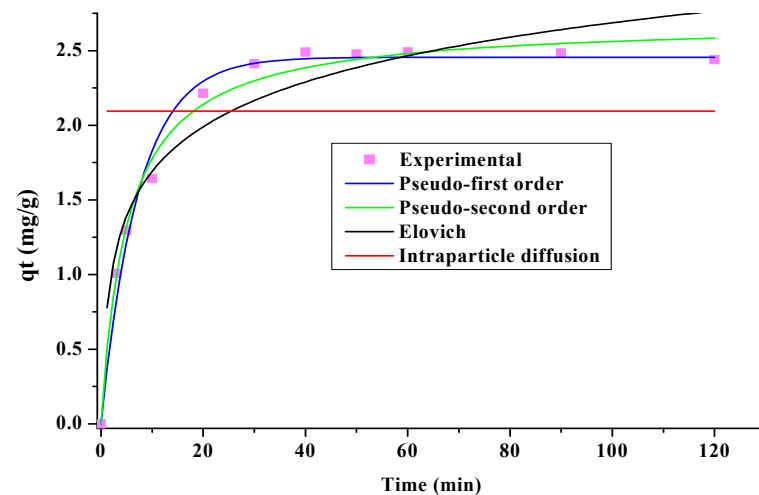
Table 3 summarizes the results of the analysis of variance with a p -value of 0.05 reliability for adsorption capacity at a 95% confidence level, where it is shown that the pH has a significantly positive effect on the ability to remove Pb (II) on eucalyptus sawdust.

Table 3. ANOVA of the effect of pH on the adsorption capacity of Pb (II).

Source	GL	Sum of Squares	Mean Square	F-Value	p Value
pH	3	24.2654	8.0885	49.98	0.000
Error	12	1.9472	0.1637		
Total	15	26.2301			

3.3. Adsorption Kinetics

The adsorption phenomenon can be controlled by different mechanisms of transfer of the contaminant from the solution to the adsorbent; thus, the kinetics establish the sequential factors involved for the metal retention to occur, such as diffusion of the metal from the solution to the surface contact area, diffusion from the surface to the pores, and the complexing of the metals, physicochemical adsorption, or chemisorption [7]. The adjustment of experimental kinetic data to pseudo-first-order, pseudo-second-order models, Elovich, and intraparticle diffusion is shown in Figure 4.

**Figure 4.** Adjustment of the adsorption kinetics of Pb (II) on eucalyptus sawdust.

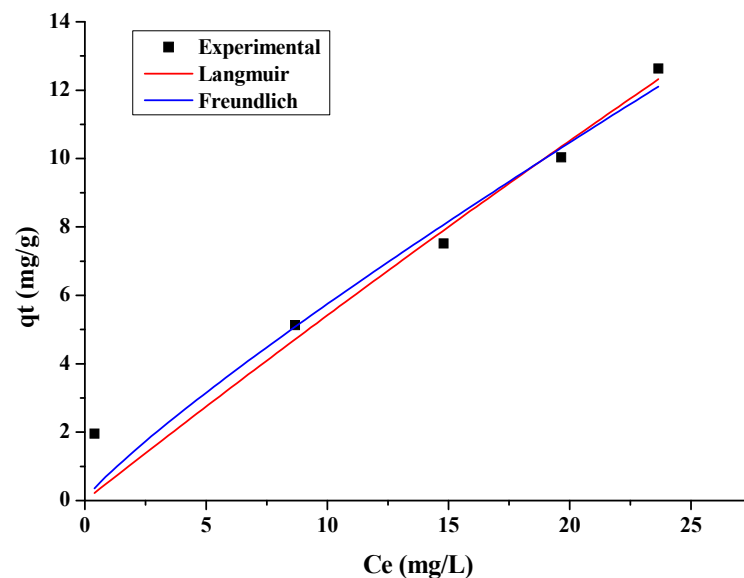
The kinetic study illustrates that the lead adsorption rate in eucalyptus sawdust had a rapid stage at the beginning, achieving maximum removal followed by a slow stage approaching equilibrium. In this study, more than 96% of the metal was adsorbed during the first 30 min, then the rate decreased, and equilibrium was reached at 50 min, the latter being established as the equilibrium time. The above indicates that, due to the occupation of the bonding centers by the metal ion, the availability of these in the sawdust is reduced [51]. From the fit of Figure 4 and the parameters summarized in Table 4, it can be said that the model that fits the experimental data is the pseudo-second-order model, which suggests that the phenomenon that controls ion adsorption in sawdust is chemical adsorption [52], and that ion retention occurs on the exposed surface of the adsorbent due to its heterogeneous nature [53]. This is evidenced by structural change after the biomaterial is placed in contact with the contaminated lead solution (Figure 2) [54].

Table 4. Adjustment parameters of sulfate adsorption kinetics.

Model	Parameters	Value
Pseudo-first-order	q_e (mg/g)	2.4561
	k_1 (min^{-1})	0.1364
	R^2	0.9859
Pseudo-second-order	q_e (mg/g)	2.69
	k_2 ($\text{g/mg} \times \text{min}$)	0.07
	R^2	0.9879
Elovich	α ($\text{mg/g} \times \text{min}$)	2.311
	β (g/mg)	2.154
	R^2	0.469
Intraparticle diffusion	k_3 ($\text{mg/g} \times \text{s}^{1/2}$)	2.09
	R^2	0.5819

3.4. Adsorption Equilibrium

Adsorption isotherm study the affinity that an adsorbent shows for a particular adsorbate [55]. In the present research, 1.5 g of cedar sawdust was set in contact with increasing concentrations of lead (30–150 mg/L) at the optimum condition of pH 6. The adsorption isotherm and the fit to Langmuir and Freundlich models of the experimental data of equilibrium of Pb (II) adsorption are shown in Figure 5. The result of the experiment showed that the metal adsorption increased consistently with increasing initial concentrations; this is explained because, at high concentrations, the concentration gradient is the flux to surpass the mass transfer resistance resulting in an improvement of the adsorption capacity [17].

**Figure 5.** Adjustment of the Pb (II) adsorption isotherm on eucalyptus sawdust.

According to the graph in Figure 5 and the parameters summarized in Table 5, it can be seen that both models fit the isotherm satisfactorily; however, the R^2 for Freundlich's model is slightly higher, which is due to the heterogeneous surface of the sawdust and the interaction of its active centers with the metal [56]. The parameter n has a value greater than 1, which confirms the heterogeneity of the bioadsorbent and denotes that adsorption is spontaneous and feasible, which is consistent with Figure 2 [57]. R_L factor refers to the separation factor; its value indicates a favorable or unfavorable adsorption procedure. R_L

> 1 is unfavorable; $R_L = 0$ is irreversible; $R_L = 1$ is linear; $0 < R_L < 1$ is favorable and feasible [58]. In Pb (II) adsorption on eucalyptus sawdust, R_L values ranged from 0.63 to 0.90, which is minus 1, indicating that the adsorption was favorable and feasible under the conditions evaluated [59].

Table 5. Adjustment parameters of sulfate adsorption isotherms.

Model	Parameter	Value
Langmuir	q_{\max} (mg/g)	145.5417
	K_L (L/mg)	0.0039
	R^2	0.9317
Freundlich	K_f (mg/g)	1.019
	N	1.288
	R^2	0.7764

4. Conclusions

The paper presented describes the efficiency of eucalyptus sawdust as a bioadsorbent material for the elimination of Pb (II) ions from a solution. The bromatological essay of the biomaterial showed a low ash content, a porous morphology with diverse texture, and the presence of fiber fragments, which describe the heterogeneity of the material. The FTIR spectrum showed the presence of amino, hydroxyl, carboxyl, aromatic, and saturated and unsaturated hydrocarbon functional groups, which are part of the structure of lignin, cellulose, hemicellulose, and pectin. From the adsorption experiments, it was obtained that the optimal pH value for the removal of the metal was determined at 6 reaching a removal percentage of 96% and an adsorption capacity of 4.80 mg/g. The adsorption kinetics followed the pseudo-second-order model and the Langmuir and Freundlich isothermal models described the adsorption equilibrium, showing that the adsorption mechanism is controlled by chemisorption through ion exchange between the metal and the active centers of the adsorbent. These results indicated that eucalyptus sawdust could be used efficiently as a cheap biosorbent for the subtraction of contaminants from the contaminated aquatic environment.

5. Novelty Statement

This manuscript entitled “Modelling the kinetics and adsorption balance of Pb (II) on residual sawdust of *Eucalyptus globulus* Labill” provides a bromatological analysis, SEM, and FTIR of the spices *Eucalyptus globulus* Labill cultivated abundantly in Huancayo, Peru. These characterizations are associated with the properties of the sawdust used for its potential implementation as an adsorbent for heavy metals such as lead. Likewise, these contributions can be used as a reference for the study of different plant species used in the wood industry and that generate residual sawdust.

In the evaluation of pH effect, we found major adsorption capacity at pH 6; this implies that, when treating real surface waters contaminated with this metal, pH corrections would not have to be made, since this is the normal average pH of surface waters.

This study could serve as the basis for the implementation of adsorption filters for the treatment of real water contaminated with lead, using sawdust as a filter bed at pH 6, taking into account the rapid adsorption rate of the adsorbent material (50 min) and its good behavior at low and high concentrations as indicated by the study of adsorption isotherms.

Author Contributions: Conceptualization, C.T.-T., A.V.-O., and H.M.-B.; data curation, A.V.-O. and R.O.-T.; formal analysis, C.T.-T. and H.M.-B.; funding acquisition, H.M.-B.; investigation H.M.-B. and F.E.-L.; methodology, C.T.-T.; project administration, H.M.-B.; resources, C.T.-T. and H.M.-B.; software, A.V.-O.; supervision, C.T.-T. and R.O.-T.; validation, C.T.-T., A.V.-O., R.O.-T., and H.M.-B.; visualization, A.V.-O.; writing—original draft, F.E.-L.; writing—review and editing, C.T.-T. and R.O.-T. All authors have read and agreed to the published version of the manuscript.

Funding: This research received no external funding.

Institutional Review Board Statement: Not applicable.

Informed Consent Statement: Not applicable.

Data Availability Statement: The data presented in this study are available upon request from the corresponding author.

Acknowledgments: The authors thank the Universidad Nacional del Centro del Perú (Perú) and the Universidad de Cartagena (Colombia) to support the development of this work regarding laboratory, software use, and time for their researchers.

Conflicts of Interest: The authors declare they have no conflict of interest.

References

1. Naseem, K.; Huma, R.; Shahbaz, A.; Jamal, J.; Rehman, M.Z.U.; Sharif, A.; Ahmed, E.; Begum, R.; Irfan, A.; Al-Sehemi, A.G.; et al. Extraction of Heavy Metals from Aqueous Medium by Husk Biomass: Adsorption Isotherm, Kinetic and Thermodynamic study. *Z. Phys. Chem.* **2018**, *233*, 201–223. [[CrossRef](#)]
2. Okoli, C.P.; Diagboya, P.N.; Anigbogu, I.O.; Olu-Owolabi, B.I.; Adebowale, K.O. Competitive biosorption of Pb(II) and Cd(II) ions from aqueous solutions using chemically modified moss biomass (*Barbula lambarenensis*). *Environ. Earth Sci.* **2017**, *76*, 33. [[CrossRef](#)]
3. Taşar, Ş.; Kaya, F.; Özer, A. Biosorption of lead(II) ions from aqueous solution by peanut shells: Equilibrium, thermodynamic and kinetic studies. *J. Environ. Chem. Eng.* **2014**, *2*, 1018–1026. [[CrossRef](#)]
4. Boskabady, M.; Marefati, N.; Farkhondeh, T.; Shakeri, F.; Farshbaf, A.; Boskabady, M.H. The effect of environmental lead exposure on human health and the contribution of inflammatory mechanisms, a review. *Environ. Int.* **2018**, *120*, 404–420. [[CrossRef](#)]
5. Bhanvase, B.A.; Ugwekar, R.P.; Mankar, R.B. (Eds.) *Novel Water Treatment and Separation Methods: Simulation of Chemical Processes*; Apple Academic Press: Waretown, NJ, USA, 2017.
6. Azimi, A.; Azari, A.; Rezakazemi, M.; Ansarpour, M. Removal of Heavy Metals from Industrial Wastewaters: A Review. *ChemBioEng. Rev.* **2017**, *4*, 37–59. [[CrossRef](#)]
7. Allahdin, O.; Mabungui, J.; Wartel, M.; Boughriet, A. Removal of Pb 2+ ions from aqueous solutions by fixed-BED column using a modified brick: (Micro)structural, electrokinetic and mechanistic aspects. *Appl. Clay Sci.* **2017**, *148*, 56–67. [[CrossRef](#)]
8. Meneguín, J.G.; Moisés, M.P.; Karchiyappan, T.; Faria, S.H.B.; Gimenes, M.L.; de Barros, M.A.S.; Venkatachalam, S. Preparation and characterization of calcium treated bentonite clay and its application for the removal of lead and cadmium ions: Adsorption and thermodynamic modeling. *Process. Saf. Environ. Prot.* **2017**, *111*, 244–252. [[CrossRef](#)]
9. Hokkanen, S.; Bhatnagar, A.; Sillanpää, M. A review on modification methods to cellulose-based adsorbents to improve adsorption capacity. *Water Res.* **2016**, *91*, 156–173. [[CrossRef](#)] [[PubMed](#)]
10. Nigam, M.; Rajoriya, S.; Singh, S.R.; Kumar, P. Adsorption of Cr (VI) ion from tannery wastewater on tea waste: Kinetics, equilibrium and thermodynamics studies. *J. Environ. Chem. Eng.* **2019**, *7*, 103188. [[CrossRef](#)]
11. Berhe, S.; Ayele, D.; Tadesse, A.; Mulu, A. Adsorption Efficiency of Coffee Husk for Removal of Lead (II) from Industrial Effluents: Equilibrium and Kinetic Study. *Int. J. Sci. Res. Publ.* **2015**, *5*, 753–859.
12. Borna, M.O.; Pirsahab, M.; Niri, M.V.; Mashizie, R.K.; Kakavandi, B.; Zare, M.R.; Asadi, A. Batch and column studies for the adsorption of chromium(VI) on low-cost Hibiscus Cannabinus kenaf, a green adsorbent. *J. Taiwan Inst. Chem. Eng.* **2016**, *68*, 80–89. [[CrossRef](#)]
13. Ijeamaka, E.C. Isotherm Studies of Adsorption of Cr (Vi) Ions onto Coconut Husk. *Int. J. Biochem. Biophys. Mol. Biol.* **2018**, *3*, 38. [[CrossRef](#)]
14. Mushtaq, M.; Bhatti, H.N.; Iqbal, M.; Noreen, S. Eriobotrya japonica seed biocomposite efficiency for copper adsorption: Isotherms, kinetics, thermodynamic and desorption studies. *J. Environ. Manag.* **2016**, *176*, 21–33. [[CrossRef](#)]
15. Naik, R.M.; Ratan, S.; Singh, I. Use of orange peel as an adsorbent for the removal of Cr (VI) from its aqueous solution. *Indian J. Chem. Technol.* **2018**, *25*, 300–305.
16. Peng, S.-H.; Wang, R.; Yang, L.-Z.; He, L.; He, X.; Liu, X. Biosorption of copper, zinc, cadmium and chromium ions from aqueous solution by natural foxtail millet shell. *Ecotoxicol. Environ. Saf.* **2018**, *165*, 61–69. [[CrossRef](#)] [[PubMed](#)]
17. Mahmood-Ul-Hassan, M.; Yasin, M.; Youssa, M.; Ahmad, R.; Sarwar, S. Kinetics, isotherms, and thermodynamic studies of lead, chromium, and cadmium bio-adsorption from aqueous solution onto Picea smithiana sawdust. *Environ. Sci. Pollut. Res.* **2018**, *25*, 12570–12578. [[CrossRef](#)]
18. Priyantha, N.; Lim, L.B.L.; Mansor, N.H.M.; Liyandeniya, A.B. Irreversible sorption of Pb(II) from aqueous solution on breadfruit peel to mitigate environmental pollution problems. *Water Sci. Technol.* **2019**, *80*, 2241–2249. [[CrossRef](#)]
19. Semerjian, L. Removal of heavy metals (Cu, Pb) from aqueous solutions using pine (*Pinus halepensis*) sawdust: Equilibrium, kinetic, and thermodynamic studies. *Environ. Technol. Innov.* **2018**, *12*, 91–103. [[CrossRef](#)]

20. Salazar-Rabago, J.; Leyva-Ramos, R. Novel biosorbent with high adsorption capacity prepared by chemical modification of white pine (*Pinus durangensis*) sawdust. Adsorption of Pb(II) from aqueous solutions. *J. Environ. Manag.* **2016**, *169*, 303–312. [CrossRef] [PubMed]
21. Demcak, S.; Balintova, M.; Hurakova, M.; Frontasyeva, M.V.; Zinicovscaia, I.; Yushin, N. Utilization of poplar wood sawdust for heavy metals removal from model solutions. *Nova Biotechnol. Chim.* **2017**, *16*, 26–31. [CrossRef]
22. Malwade, K.; Lataye, D.; Mhaisalkar, V.; Kurwadkar, S.; Ramirez, D. Adsorption of hexavalent chromium onto activated carbon derived from *Leucaena leucocephala* waste sawdust: Kinetics, equilibrium and thermodynamics. *Int. J. Environ. Sci. Technol.* **2016**, *13*, 2107–2116. [CrossRef]
23. Sahmoune, M.N.; Yeddou, A.R. Potential of sawdust materials for the removal of dyes and heavy metals: Examination of isotherms and kinetics. *Desalination Water Treat.* **2016**, *57*, 24019–24034. [CrossRef]
24. Valverde, J.C.; Barrera, V.M.; Guillén, R. Estimación de la biomasa aérea de *Eucalyptus globulus* Labill plantado en cercos vivos, distrito Huertas, Junín (Perú). *Rev. For. Perú* **2019**, *34*, 52–65. [CrossRef]
25. FAO. FAO of the U.N. and Instituto Tecnológico de la Producción (ITP)-CITEmadera *La Industria de la Madera en el Perú*. Lima. 2018. [Online]. Available online: <http://www.fao.org/3/I8335ES/i8335es.pdf> (accessed on 20 March 2021).
26. Villabona-Ortiz, A.; De Cartagena, U.; Tejada-Tovar, C.N.; Ortega-Toro, R. Modelling of the Adsorption Kinetics of Chromium (vi) Using Waste Biomaterials. *Rev. Mex. Ing. Química* **2019**, *19*, 401–408. [CrossRef]
27. Mahdi, Z.; Yu, Q.J.; El Hanandeh, A. Competitive adsorption of heavy metal ions (Pb²⁺, Cu²⁺, and Ni²⁺) onto date seed biochar: Batch and fixed bed experiments. *Sep. Sci. Technol.* **2018**, *54*, 888–901. [CrossRef]
28. Singh, Y.D.; Mahanta, P.; Bora, U. Comprehensive characterization of lignocellulosic biomass through proximate, ultimate and compositional analysis for bioenergy production. *Renew. Energy* **2017**, *103*, 490–500. [CrossRef]
29. Cai, J.; He, Y.; Yu, X.; Banks, S.W.; Yang, Y.; Zhang, X.; Yu, Y.; Liu, R.; Bridgwater, A.V. Review of physicochemical properties and analytical characterization of lignocellulosic biomass. *Renew. Sustain. Energy Rev.* **2017**, *76*, 309–322. [CrossRef]
30. Aiyesanmi, A.F.; Adebayo, M.A.; Arowojobe, Y. Biosorption of Lead and Cadmium from Aqueous Solution in Single and Binary Systems Using Avocado Pear Exocarp: Effects of Competing Ions. *Anal. Lett.* **2020**, *53*, 2868–2885. [CrossRef]
31. El-Azazy, M.; El-Shafie, A.S.; Issa, A.A.; Al-Sulaiti, M.; Al-Yafie, J.; Shomar, B.; Al-Saad, K. Potato Peels as an Adsorbent for Heavy Metals from Aqueous Solutions: Eco-Structuring of a Green Adsorbent Operating Plackett–Burman Design. *J. Chem.* **2019**, *2019*, 1–14. [CrossRef]
32. Tejada-Tovar, C.; Gonzalez-Delgado, A.D.; Villabona-Ortiz, A. Characterization of Residual Biomasses and Its Application for the Removal of Lead Ions from Aqueous Solution. *Appl. Sci.* **2019**, *9*, 4486. [CrossRef]
33. Al-Lagtah, N.M.; Al-Muhtaseb, A.H.; Ahmad, M.N.; Salameh, Y. Chemical and physical characteristics of optimal synthesised activated carbons from grass-derived sulfonated lignin versus commercial activated carbons. *Microporous Mesoporous Mater.* **2016**, *225*, 504–514. [CrossRef]
34. Manirethan, V.; Gupta, N.; Balakrishnan, R.M.; Raval, K. Batch and continuous studies on the removal of heavy metals from aqueous solution using biosynthesised melanin-coated PVDF membranes. *Environ. Sci. Pollut. Res.* **2019**, *27*, 24723–24737. [CrossRef]
35. Rinaldi, R.; Yasdi, Y.; Hutagalung, W.L.C. Removal of Ni (II) and Cu (II) ions from aqueous solution using rambutan fruit peels (*Nephelium lappaceum* L.) as adsorbent. In Proceedings of the Fourth Huntsville Gamma-Ray Burst Symposium; AIP Publishing: Yogyakarta, Indonesia August 14 and 15. , 2018; Volume 2026, p. 020098.
36. Amro, A.N.; Abhary, M.K.; Shaikh, M.M.; Ali, S. Removal of Lead and Cadmium Ions from Aqueous Solution by Adsorption on a Low-Cost Phragmites Biomass. *Processes* **2019**, *7*, 406. [CrossRef]
37. Guedidi, H.; Reinert, L.; Soneda, Y.; Bellakhal, N.; Duclaux, L. Adsorption of ibuprofen from aqueous solution on chemically surface-modified activated carbon cloths. *Arab. J. Chem.* **2017**, *10*, S3584–S3594. [CrossRef]
38. Asuquo, E.D.; Martin, A.D. Sorption of cadmium (II) ion from aqueous solution onto sweet potato (*Ipomoea batatas* L.) peel adsorbent: Characterisation, kinetic and isotherm studies. *J. Environ. Chem. Eng.* **2016**, *4*, 4207–4228. [CrossRef]
39. Feizi, M.; Jalali, M. Removal of heavy metals from aqueous solutions using sunflower, potato, canola and walnut shell residues. *J. Taiwan Inst. Chem. Eng.* **2015**, *54*, 125–136. [CrossRef]
40. Wang, X.; Wang, L.; Wang, Y.; Tan, R.; Ke, X.; Zhou, X.; Geng, J.; Hou, H.; Zhou, M. Calcium Sulfate Hemihydrate Whiskers Obtained from Flue Gas Desulfurization Gypsum and Used for the Adsorption Removal of Lead. *Crystals* **2017**, *7*, 270. [CrossRef]
41. Powell, K.J.; Brown, P.L.; Byrne, R.H.; Gajda, T.; Hefter, G.; Leuz, A.-K.; Sjöberg, S.; Wanner, H. Chemical speciation of environmentally significant metals with inorganic ligands. Part 3: The Pb²⁺ + OH⁻, Cl⁻, CO₃²⁻, SO₄²⁻, and PO₄³⁻ systems (IUPAC Technical Report). *Pure Appl. Chem.* **2009**, *81*, 2425–2476. [CrossRef]
42. Basu, M.; Guha, A.K.; Ray, L. Adsorption of Lead on Cucumber Peel. *J. Clean. Prod.* **2017**, *151*, 603–615. [CrossRef]
43. Chi, T.; Zuo, J.; Liu, F. Performance and mechanism for cadmium and lead adsorption from water and soil by corn straw biochar. *Front. Environ. Sci. Eng.* **2017**, *11*, 15. [CrossRef]
44. Saad, A.A.; Amer, R.A.; Tayeb, E.H.; Nady, N.; Mohamed, R.G. Unmodified Rice Straw for The Lead Removal Approach from Synthetic Lead Solution. *Alex. Sci. Exch. J.* **2020**, *41*, 43–52. [CrossRef]
45. Alhogbi, B.G.; Salam, M.A.; Ibrahim, O. Environmental remediation of toxic lead ions from aqueous solution using palm tree waste fibers biosorbent. *Desalination Water Treat.* **2019**, *145*, 179–188. [CrossRef]

46. Putra, W.P.; Kamari, A.; Yusoff, S.N.M.; Ishak, C.F.; Mohamed, A.; Hashim, N.; Isa, I.M. Biosorption of Cu(II), Pb(II) and Zn(II) Ions from Aqueous Solutions Using Selected Waste Materials: Adsorption and Characterisation Studies. *J. Encapsul. Adsorpt. Sci.* **2014**, *4*, 25–35. [[CrossRef](#)]
47. Olasehinde, E.F.; Adegunloye, A.V.; Adebayo, M.A.; Oshodi, A.A. Sequestration of Aqueous Lead(II) Using Modified and Unmodified Red Onion Skin. *Anal. Lett.* **2018**, *51*, 2710–2732. [[CrossRef](#)]
48. Kariuki, Z.; Kiptoo, J.; Onyancha, D. Biosorption studies of lead and copper using rogers mushroom biomass 'Lepiota hystrix'. *S. Afr. J. Chem. Eng.* **2017**, *23*, 62–70. [[CrossRef](#)]
49. Alorabi, A.Q.; Alharthi, F.A.; Azizi, M.; Al-Zaqri, N.; El-Marghany, A.; Abdelshafeek, K.A. Removal of Lead(II) from Synthetic Wastewater by *Lavandula pubescens* Decne Biosorbent: Insight into Composition–Adsorption Relationship. *Appl. Sci.* **2020**, *10*, 7450. [[CrossRef](#)]
50. Rozman, U.; Kalčíková, G.; Marolt, G.; Skalar, T.; Gotvajn, A. Žgajnar Potential of waste fungal biomass for lead and cadmium removal: Characterization, biosorption kinetic and isotherm studies. *Environ. Technol. Innov.* **2020**, *18*, 100742. [[CrossRef](#)]
51. Kaur, M.; Kumari, S.; Sharma, P. Removal of Pb (II) from aqueous solution using nanoadsorbent of *Oryza sativa* husk: Isotherm, kinetic and thermodynamic studies. *Biotechnol. Rep.* **2020**, *25*, e00410. [[CrossRef](#)] [[PubMed](#)]
52. Obike, A.; Igwe, J.; Emeruwa, C.; Uwakwe, K. Equilibrium and kinetic studies of Cu (II), Cd (II), Pb (II) and Fe (II) adsorption from aqueous solution using cocoa (*Theobroma cacao*) pod husk. *J. Appl. Sci. Environ. Manag.* **2018**, *22*, 182. [[CrossRef](#)]
53. Asuquo, E.; Martin, A.; Nzerem, P.; Siperstein, F.; Fan, X. Adsorption of Cd(II) and Pb(II) ions from aqueous solutions using mesoporous activated carbon adsorbent: Equilibrium, kinetics and characterisation studies. *J. Environ. Chem. Eng.* **2017**, *5*, 679–698. [[CrossRef](#)]
54. Haq, A.U.; Saeed, M.; Anjum, S.; Bokhari, T.H.; Usman, M.; Tubbsum, S. Evaluation of Sorption Mechanism of Pb (II) and Ni (II) onto Pea (*Pisum sativum*) Peels. *J. Oleo Sci.* **2017**, *66*, 735–743. [[CrossRef](#)] [[PubMed](#)]
55. Raikar, R.V.; Correa, S.; Ghorpade, P. Removal of lead (II) from aqueous solution using natural and activated rice husk. *Int. Res. J. Eng. Technol.* **2015**, *2*, 1677–1686.
56. Perez, T.; Pasquini, D.; Lima, A.D.F.; Rosa, E.V.; Sousa, M.H.; Cerqueira, D.A.; De Moraes, L.C. Efficient removal of lead ions from water by magnetic nanosorbents based on manganese ferrite nanoparticles capped with thin layers of modified biopolymers. *J. Environ. Chem. Eng.* **2019**, *7*, 102892. [[CrossRef](#)]
57. Ibisi, N.; Asoluka, C. Use of agro-waste (*Musa paradisiaca* peels) as a sustainable biosorbent for toxic metal ions removal from contaminated water. *Chem. Int.* **2018**, *4*, 52–59. Available online: <http://bosajournals.com/chemint/images/pdffiles/18-7.pdf> (accessed on 20 March 2021).
58. Abiazem, C.V.; Williams, A.B.; Inegbenebor, A.I.; Onwordi, C.T.; Ehi-Eromosele, C.O.; Petrik, L.F. Adsorption of lead ion from aqueous solution onto cellulose nanocrystal from cassava peel. *J. Phys. Conf. Ser.* **2019**, *1299*, 012122. [[CrossRef](#)]
59. Yu, X.-L.; He, Y. Optimal ranges of variables for an effective adsorption of lead (II) by the agricultural waste pomelo (*Citrus grandis*) peels using Doehlert designs. *Sci. Rep.* **2018**, *8*, 729. [[CrossRef](#)] [[PubMed](#)]